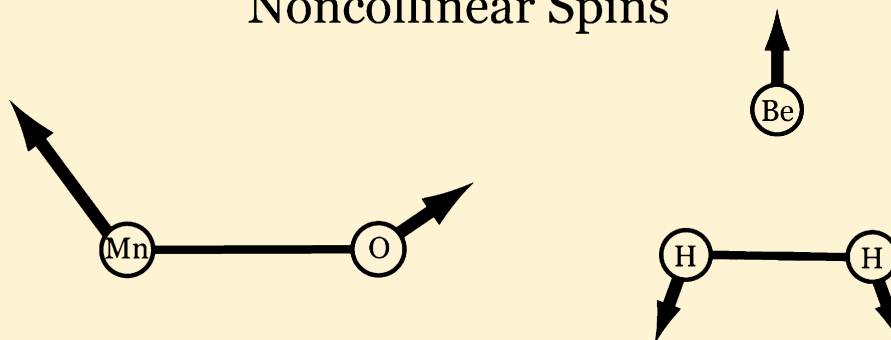


Noncollinear Spin States for Density Functional Calculations of Open-Shell and Multi-Configurational Systems: Dissociation of MnO and NiO and Barrier Heights of O₃, BeH₂, and H₄

Sijie Luo and Donald G. Truhlar*

Department of Chemistry, Supercomputing Institute, and Chemical Theory Center, University of Minnesota, Minneapolis, Minnesota 55455-0431, United States

Noncollinear Spins



ABSTRACT: When the spins of molecular orbitals are allowed to be aligned with different directions in space rather than being aligned collinearly, the resulting noncollinear spin orbitals add extra flexibility to variational optimization of the orbitals, and solutions obtained with collinear spin orbitals may be unstable with respect to becoming noncollinear in the expanded variational space. The goal of the present work is to explore whether and in what way the molecular orbitals of the Kohn–Sham density functional theory become noncollinear when fully optimized for multi-reference molecules, transition states, and reaction paths. (We note that a noncollinear determinant has intermediate flexibility between a collinear determinant and a linear combination of many collinear determinants with completely independent coefficients. However, the Kohn–Sham method is defined to involve the variational optimization of a single determinant, and a noncollinear determinant represents the limit of complete optimization in the Kohn–Sham scheme.) We compare the results obtained with the noncollinear Kohn–Sham (NKS) scheme to those obtained with the widely used unrestricted Kohn–Sham (UKS) scheme for two types of multi-reference systems. For the dissociation of the MnO and NiO transition metal oxides, we find UKS fails to dissociate to the ground states of neutral atoms, while NKS dissociates to the correct limit and predicts potential energy curves that vary smoothly at intermediate bond lengths. This is due to the instability of UKS solutions at large bond distances. For barrier heights of O₃, BeH₂, and H₄, NKS is shown to stabilize the multi-reference transition states by expanding the variational space. Although the errors vary because they are closely coupled with the capability of the employed exchange–correlation functionals in treating the multi-configurational states, these findings demonstrate that results with collinear spin orbitals should be further scrutinized, and future development of exchange–correlation functionals for multi-reference systems should incorporate the flexibilities of NKS.

1. INTRODUCTION

Kohn–Sham density functional theory¹ is based on representing electron density as the square magnitude of a single Slater determinant. The energy is computed by a variational principle in which the energy is minimized with respect to variations of the orbitals in the Slater determinant. However, the Slater determinant is not a wave function for the real system (it is a wave function for a system with the same density as the real system but with noninteracting electrons), and consequently, one should not overinterpret the Slater determinant. For example, it is not required to have the correct expectation value of the spin density or of \hat{S}^2 , where \hat{S} is total electron spin.² Therefore, the variational determination of the ground-state

energy should be carried out without spin or symmetry constraints in the Slater determinant.³

In wave function theory, it is very convenient to use symmetry-adapted configuration state functions that are linear combinations of Slater determinants. Because one can use multiple Slater determinants, it is not a restriction to take the spin–orbitals used in the Slater determinants as collinear, i.e., to have the form of a spatial function times spin function α or spin function β , where α and β are quantized along a single arbitrary laboratory-fixed axis. When one is restricted to a single determinant, as in Hartree–Fock theory or Kohn–Sham

Received: August 24, 2013

Published: November 19, 2013



density functional theory, though, this is a restriction; and an unconstrained variational optimization should allow each spin-orbital ψ_j to be an arbitrary linear combination

$$\psi_j = \phi_{j1}(\mathbf{r})\alpha + \phi_{j2}(\mathbf{r})\beta \quad (1)$$

where ϕ_{ji} is a complex spatial function, and ψ_j is called a general spin-orbital (GSO). General spin-orbitals arise naturally in relativistic wave function theory and relativistic density functional theory, where they may be used to treat spin-orbit coupling.^{4–6} They have also been employed with the Hartree–Fock wave function method, where the result is called generalized Hartree–Fock^{7–9} and with nonrelativistic (or single-component scalar relativistic) density functional theory,^{10–28} where the result is usually called noncollinear Kohn–Sham (NKS) theory. Most NKS calculations reported so far have been used to study magnetic solids and unligated and ligated metal clusters formed by transition metals.^{10–12,16,23,26} Here, we present some examples to show their usefulness for diatomic molecule potential curves and for three systems with no transition metals but with significant multi-configurational character. In particular, we present calculations on MO ($M = \text{Mn}, \text{Ni}$), O_3 , H_4 , and BeH_2 . The goal of the paper is to learn whether noncollinear solutions are more stable than collinear ones for a variety of kinds of multi-reference systems, to see if the noncollinear solutions yield smoother potential energy curves or significantly different reaction barriers, and to illustrate the orientations of the noncollinear spin vectors in some cases.

From the point of view of wave function theory, for example, from the point of view of generalized Hartree–Fock theory, we note that a noncollinear determinant can be rewritten as a linear combination of collinear ones, and optimizing a noncollinear determinant may be considered to provide a limited optimization of multi-determinantal character. While the noncollinear determinant has more variational flexibility than a collinear determinant, it has less flexibility than a linear combination of many collinear determinants with completely independent coefficients. However, from the point of view of Kohn–Sham density functional theory, a noncollinear determinant plays a more canonical role. In particular, the Kohn–Sham method is defined to involve the variational optimization of a single determinant, and a noncollinear determinant represents the limit of complete optimization in the general case, although in specific cases the variationally optimized determinant might correspond to the special case of a collinear determinant. The examples in the present article will show both kinds of cases, that is, cases where the collinear determinant is stable and cases where it is not.

We will use the following notation. Complete optimization of the Slater determinant with GSOs will be called NKS. Optimization with the restriction to collinear spin-orbitals will be called unrestricted Kohn–Sham (UKS), analogous to unrestricted Hartree–Fock. We note that this kind of optimization is often simply called the broken-symmetry method, but this term can be ambiguous because it usually refers to a multi-step process for extracting an energy estimate from the broken-symmetry solutions. Furthermore, the NKS solution may also break symmetry. UKS, although it usually breaks spatial symmetry (if present), makes the Slater determinant an eigenfunction of \hat{S}_z with eigenvalue M_S but does not give eigenfunctions of \hat{S}^2 . Optimization with the restrictions of (i) collinear spin-orbitals, (ii) eigenfunctions of

\hat{S}^2 with $M_S = S > 0$, (iii) $2M_S$ singly occupied orbitals, and (iv) the rest of the orbitals doubly occupied may be called restricted open-shell Kohn–Sham; this is not recommended and is not employed here. Finally, we will use the shorthand term “multi-reference” to denote systems that require more than one symmetry-adapted configuration state function for an adequate treatment by wave function theory, as reviewed elsewhere.²⁹

2. SYSTEMS

Bond dissociations of metal oxide diatomics provide some of the simplest examples of a process that cannot be treated adequately by UKS. Consider, e.g., MnO . The ground state has $S = 5/2$, and so UKS would involve a determinant with $M_S = 5/2$. But the ground states of the dissociation products are $\text{Mn}(S = 5/2)$ and $\text{O}(S = 1)$. To treat this with an unrestricted but collinear single Slater determinant would require a determinant with $M_S = 7/2$ or a determinant with $M_S = 3/2$. Similarly, $\text{NiO}(S = 1)$ should dissociate to $\text{Ni}(S = 1)$ plus $\text{O}(S = 1)$, which requires $M_S = 1$ at the equilibrium geometry and $M_S = 2$ at the dissociation limit. In this article, we will examine the foolowing question: Can NKS treat this kind of potential curve qualitatively correctly?

Next, we will consider three examples that do not involve a transition metal or a dissociation process but rather contain multi-configurational transition states: (a) The potential energy surface of ozone. Ozone, although it is a closed-shell singlet, is a classic example of a problem that profits in wave function theory from a multi-configurational self-consistent field treatment.^{30–35} In particular, ozone has significant biradical character, which is best described in wave function theory by mixing doubly excited configurations with the dominant configuration. (b) Insertion of Be into H_2 . This is another popular test for handling multi-reference character.³⁶ (c) H_4 , which also has been widely used to test the ability of various quantum chemistry methods in treating multi-reference character.³⁷ In the present study, we are comparing the energy difference between a TS of square geometry with four H–H distances of 2.0 bohrs, and a lower-energy geometry with three identical H–H distances of 2.0 bohrs. Here we ask the following: Can NKS provide an improved description of these multi-configurational transition states relative to UKS?

3. METHODS

All the DFT calculations were performed with a locally modified version of VASP 5.3^{38,39} using the projector augmented wave (PAW)⁴⁰ method and either the PBE⁴⁵ or the PBE0⁴³ exchange–correlation functional. (The functionals are used without modification, and the local modifications of VASP are not required for the present calculations.) Because VASP does not provide PAW potentials for each exchange–correlation functional, we used the latest PAW potentials generated from the PBE functional, which can be downloaded from the VASP Web site; these potentials also contain the kinetic energy densities, which are necessary for meta-GGA calculations. The unit cell is of size $10 \text{ \AA} \times 11 \text{ \AA} \times 12 \text{ \AA}$, and the cutoff energy is 1000 eV. It has been shown previously that VASP calculations using PAW potentials are able to reproduce DFT calculations using high-quality Gaussian-type basis sets,⁴¹ and our tests also showed that collinear DFT results obtained from VASP and *Gaussian 09* agree within 0.5 kcal/mol.

In carrying out the calculations, we found it essential to use the feature in VASP that allows one to initialize the SCF

iterations with a determinant that breaks the spin symmetry in an appropriate way. This is achieved in VASP by specifying the initial spin magnetic moment on each atom.

For ozone, we carried out complete-active-space second-order perturbation⁴² (CASPT2) calculations with Molpro^{47,48} with 12 electrons in 9 active orbitals and the aug-cc-pV5Z basis set to optimize the geometries of both ozone and cyclic ozone, and we obtained 12 intermediate geometries (Table 1) by

Table 1. Energies Changes (kcal/mol) from Cyclic Ozone ($\alpha = 1.0$) to Ozone ($\alpha = 0.0$) Calculated by UKS and NKS with PBE and PBE0 with $M_S = 0$

λ	CASPT2	UPBE	NPBE	UPBE0	NPBE0
1 ^a	0	0	0	0	0
0.9 ^b	1.9	2.2	2.2	2.4	2.4
0.8	6.8	8.1	8.1	8.4	8.3
0.75	10.3	12.9	12.0	12.5	12.0
0.7	14	16.6	13.5	16.2	15.0
0.65	19.5	14.6	11.8	14.2	12.5
0.6	22.8	7.3	7.1	9.4	4.6
0.55	21.7	2.9	2.7	4.3	0.0
0.5	19.3	-1.4	-1.6	0.2	-4.5
0.4	-1.0	-4.0	-5.8	-3.6	-7.6
0.3	-16	-14.9	-15.2	-17.5	-17.5
0.2	-26.2	-26.7	-26.7	-26.8	-26.8
0.1	-31.9	-33.6	-33.6	-31.9	-31.9
0 ^c	-33.8	-36.4	-36.4	-33.1	-33.1

^aEquilateral triangle with $R(\text{O}-\text{O}) = 1.448 \text{ \AA}$ and bond angle equal to 60° . ^bCentral oxygen atom is located at the origin, and the Cartesian coordinates of the other two atoms are $(-x|\lambda), (y|\lambda), 0$ and $(x|\lambda), (y|\lambda), 0$. Here, $(q|\lambda) = (q|\lambda=0) + \lambda[(q|\lambda=1) - (q|\lambda=0)]$, where $q = x$ or y . In \AA , $(x|\lambda=0) = 1.091$, $(x|\lambda=1) = 0.724$, $(y|\lambda=0) = 0.674$, $(y|\lambda=1) = 1.254$. ^c $R(\text{O}-\text{O})$ is 1.282 \AA , and the bond angle equals 116.6° .

linear interpolation. Single-point CASPT2 calculations were then performed to construct the reference potential energy curve, providing a test case of a reaction profile with a barrier. For H_4 and BeH_2 , the geometries used for the calculations and the reference barrier heights in Table 2 are taken from previous studies.^{36,37}

Table 2. Barrier Heights for Insertion of Be into H_2 (kcal/mol) Calculated by UKS and NKS with PBE and PBE0 with $M_S = 0$

	UKS	NKS
PBE	100.9	87.6
PBE0	91.8	83.4
ref	114.7 ^a	

^aFrom ref 36.

4. RESULTS

4.1. MnO and NiO Dissociation. We first performed calculations on two transition metal oxides using the PBE0 exchange–correlation functional, and the results are given in Figures 1 and 2. Figure 1 compares the dissociation curves of MnO obtained by UKS (for $M_S = 5/2$ and $7/2$) to that obtained by NKS. The zero of energy is taken as the sum of energies of the two atoms in their ground states (sextet for Mn and triplet for O). First, we consider the two UKS calculations.

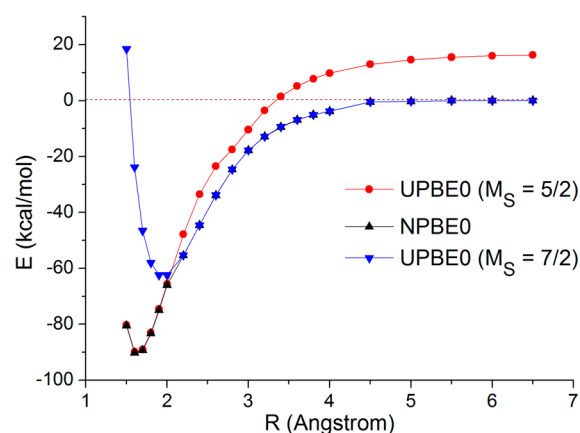


Figure 1. Dissociation curve of MnO calculated with PBE0 using UKS and NKS. The NKS curve corresponds to $M_S = 5/2$.

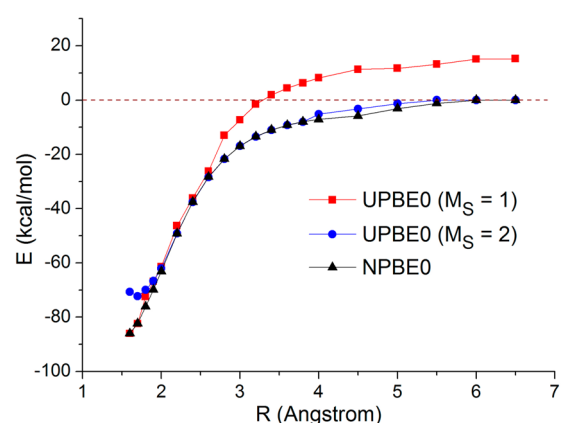


Figure 2. Dissociation curve of NiO calculated with PBE0 using UKS and NKS. The NKS curve corresponds to $M_S = 1$.

Near equilibrium, the ground state of MnO is a sextet, which, however, dissociates to a wrong limit composed of a sextet Mn and a singlet O. This limit is about 20 kcal/mol higher than the correct one, and the error is precisely equal to the triplet–singlet gap of the oxygen atom calculated by PBE0. The error originates from the fact that to correctly describe an isolated sextet Mn atom together with an isolated triplet atom with a single Slater determinant within the collinear spin scheme the determinant must have $M_S = 7/2$. This, however, contradicts the requirement of $M_S = 5/2$ to treat the ground state near equilibrium. The above can be verified by examining the UKS curve (also shown in Figure 1) for the octet state of MnO, which is the excited state near equilibrium, but correctly dissociates to the limit of $\text{Mn}(S = 5/2) + \text{O}(S = 1)$. Thus, UKS is intrinsically incapable of describing the spin coupling through the process of dissociation. Although one may attempt to describe the dissociation behavior by combining the two UKS curves, the merged results fail to provide any insight into the intermediate region, which in real applications is often the most chemically important one for reaction mechanism or catalysis studies.

Next, we consider the NKS curve. It is clear that by relaxing the constraint of collinear spins, the resulting Kohn–Sham orbitals have more flexibility to describe the whole energy curve. Because no constraints on spin states are present in our NKS calculations, the SCF iterations can converge to the lowest-energy state. Hence, near equilibrium NKS delivers

results identical to the $M_S = 5/2$ UKS calculation, while at long bond lengths, it also correctly predicts the dissociation behavior. Also notable is the smooth transition at intermediate bond lengths from the sextet to the octet. This shows that NKS can describe the dissociation of this transition metal system smoothly along the whole reaction path.

We note that the NKS calculations are not automatic. During our attempt to locate the lowest-energy solution, we found that an NKS calculation initiated with a UKS configuration would generally stay in the UKS variational space without further spin symmetry breaking. Only when the initial guess properly breaks the symmetry would the SCF successfully converge to a real NKS solution. We did find, however, that once the symmetry is broken, the SCF iterations would usually converge to the same NKS solution, regardless the specific spin configuration in use.

By comparing the local spin magnetic moments on each atom, we obtain additional insights relevant to the goal of illustrating the orientations of the noncollinear spin vectors in some cases where the molecular orbitals of Kohn–Sham density functional theory become noncollinear when fully optimized. The atomic magnetic moments are defined by integration of the magnetization over the space within a certain radius around the atoms. (Thus, these moments are not equal to expectation values of spin operators. The normalization is such that the magnetic moment of a single electron would be $2m_B$, i.e., unity rather than one-half.) Parts (a) and (b) of Figure 3 provide these atomic magnetic moments for MnO at an

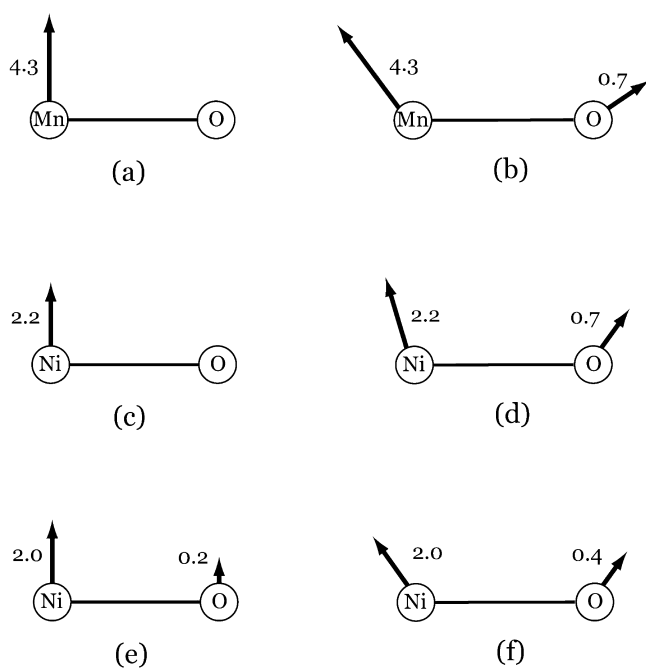


Figure 3. Local spin magnetic moments calculated by PBE0. Bond distances of 6.0 Å: (a) MnO by UKS with $M_S = 5/2$, (b) MnO by NKS, (c) NiO by UKS with $M_S = 1$, and (d) NiO by NKS. Bond distances of 4.5 Å: (e) NiO by UKS with $M_S = 1$ and (f) NiO by NKS.

internuclear distance of 6 Å. Parts (a) and (b) in Figure 3 compare the MnO results obtained by UKS and NKS. The UKS results clearly show that at the dissociation limit the magnitude of the local spin magnetic moment on the Mn atom is 4.2, approximately consistent with that of a sextet state ($2S = 5$); it also shows that the O atom is in the singlet state rather than the triplet state, verifying the deficiency of collinear spins.

This intrinsic difficulty is alleviated in NKS by relaxing the spins as shown in (b), and both Mn and O atoms are in their ground state, while remaining describable by a single determinant of $M_S = 5/2$. Notice that parts (a) and (b) of Figure 3 both correspond to $M_S = 5/2$, and yet the solutions differ in energy by 20 kcal/mol. This is a clear demonstration of the dependence of the energy on the relaxing of the collinear constraint. (The magnetic moments in Figure 3 serve as pictorial aids to illustrate how NKS relaxes the spin collinearity constraint to achieve the lowest-energy broken-symmetry SCF solution, but they do not describe the physical situation, just as the UKS polarized spin densities on each hydrogen atom for the dissociated H_2 molecule do not describe experimental observables.)

Similar results for dissociation curves are observed in Figure 2, comparing the UKS and NKS dissociation curves for NiO. For bond distances of 4.0 to 5.5 Å, we also find that NKS leads to a solution that is slightly lower in energy than the UKS one. This implies that NKS not only offers extra variational freedom for the NiO system to avoid spin frustration, but also it leads to a slightly different SCF solution that is not located within the UKS variational space. The local magnetic moments are drawn for NiO at bond distances of 6.0 Å in Figure 3 (c) and (d) and at bond distances of 4.5 Å in Figure 3 (e) and (f).

These are just two examples of the kind of transition-metal-containing systems with complicated spin states that are problematic for collinear KS. These systems could include metal dimers, metal clusters, and oxo-metal cores in important metal–organic species. As we previously showed,²⁶ NKS can provide new possibilities in modeling the complicated low-lying spin states with both computational convenience and theoretical simplicity.

NKS does not always lead to a lower-energy SCF solution than UKS because the variational space of UKS is essentially completely contained in that of NKS. We consider, for example, MnO. One can observe that for bond distances of 1.5 to 2.0 Å the NKS solution exactly matches the UKS solution, implying that the UKS treatment is sufficient. Nevertheless, without an NKS calculation or a stability test of the UKS solution, one could not predict the stability in advance, and thus, an NKS calculation or a stability analysis is required to demonstrate attainment of the variational minimum energy. (Because the generalized Hartree–Fock theory (GHF) also uses noncollinear spin orbitals, it can lead to qualitatively similar results as those obtained by NKS. GHF has been discussed in various places in the literature, but these studies did not approach the problem of noncollinear spin orbitals from the same perspective as used here. We did not pursue this issue for GHF, because due to not having a correlation functional, GHF is quantitatively wrong for descriptions of the systems discussed in this paper.)

4.2. Barrier Heights of Ozone, BeH_2 , and H_4 . Now, we turn to several systems without transition metals, starting by considering ozone. It is well known that a cyclic high-energy structure exists for ozone, and by considering a linear synchronous path⁴⁴ parametrized by the progress variable λ between normal and cyclic ozone, we can test the ability of UKS and NKS to handle highly multi-configurational systems. The results are compared in Table 1 and Figure 4, tabulating the energy changes along the path from the high-energy cyclic ozone ($\lambda = 1.0$) to the low-energy normal ozone ($\lambda = 0.0$). First, consider the UKS results with the PBE⁴⁵ exchange–correlation functional; these calculations yield a barrier height 6

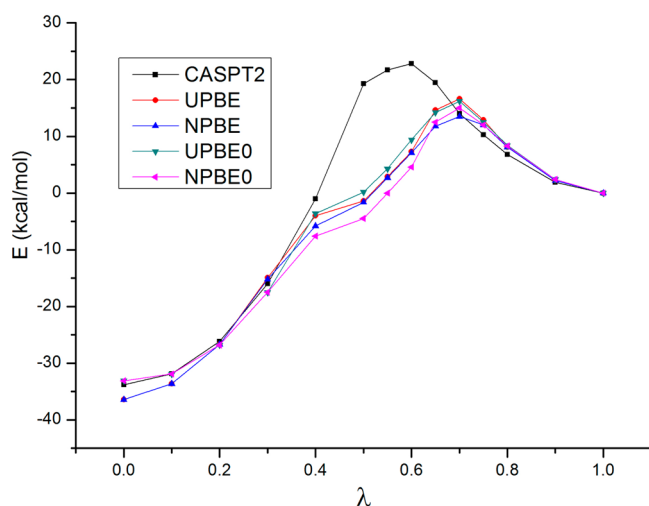


Figure 4. Energies changes (kcal/mol) from cyclic ozone ($x = 1.0$) to ozone ($x = 0.0$) calculated by UKS and NKS with PBE and PBE0 with $M_S = 0$.

kcal/mol lower than the CASPT2 barrier. This is no surprise because generalized gradient approximations like PBE are well known to underestimate barrier heights.⁴⁹ However, we also find that PBE0, with a 25% Hartree–Fock exchange, offers no improvement. Next, we turn to NKS. We find no energy lowering for either the normal ozone or the cyclic one when collinear spins are allowed to relax. However, for PBE, one finds an energy lowering of 0.1 to 3.1 kcal/mol in intermediate structures with $\lambda = 0.3$ to 0.7. Similar energy lowering is also observed for PBE0 results in the λ range from 0.5 to 0.8, with the magnitude ranging from 0.1 to 4.8 kcal/mol. Thus, the more complete variational optimization of the Slater determinant changes the shape of the calculated reaction barrier. Because UKS already underestimates the barrier height, NKS results present even larger errors by further stabilizing the transition states. So, if we were to judge the accuracy of the exchange–correlation functionals for this multi-reference system by comparison to the reference values, one would draw an incorrect conclusion. Despite the larger error of NKS with the exchange–correlation functionals employed here, it provides a more stabilized SCF solution. The most stabilized solution would provide the correct prediction if the unknown exact exchange–correlation functional were used, and the resulting exact SCF solution would be NKS-stable. Thus, if better agreement with the experiment is obtained by imposing symmetry constraints on the spin orbitals, it just represents cancellation of errors due to the exchange–correlation functional with those due to incomplete optimization. In the long term, we would prefer to use exchange–correlation functionals designed to give good results with full variational optimization. However, at this moment, we are limited to GGA and hybrid GGA functionals due to the present lack of software capable of performing NKS with completely general functionals, e.g., with meta-GGA functionals. To facilitate understanding of the PBE noncollinear results in Figure 4 and Table 1, we calculated the magnetic moments on each oxygen atom for the transition state ($\lambda = 0.7$) as shown in Figure 5 (a) and (b). These figures show that by using noncollinear spin orbitals, the system is able to be variationally stabilized to avoid spin frustration due to spin collinearity constraints.

Next, we consider another system with a multi-reference transition state, namely, the insertion of Be into H_2 . The results are tabulated in Table 2, showing that the most stable UKS results obtained by PBE and PBE0 underestimate the barrier heights by 14.7 and 22.9 kcal/mol, respectively; this again contradicts the common expectation that hybrid GGAs predict higher barrier heights than GGAs. In this case, one observes a further stabilization of 13.3 and 8.4 kcal/mol with NKS for PBE and PBE0, respectively. The large stabilization by use of noncollinear spins should further be considered in combination with the fact that most widely popular exchange–correlation functionals were previously designed and tested with collinear-spin Kohn–Sham orbitals. To advance the development of better functionals, many of the multi-configurational systems need to be reexamined with greater attention to the stability of the solutions of the Kohn–Sham equations. By comparing the local magnetic moments on each atom in Figure 5 (c) and (d), one sees that the local spin on two hydrogen atoms are further relaxed to align noncollinearly with PBE NKS calculations.

As a third example, we show a system where NKS, even with the presently available functionals, leads to both more stabilized states and better accuracy. The energy differences between square and linear H_4 , a widely used test model for treating multi-reference systems, are shown in Table 3. UKS gives similar results for PBE and PBE0, with barrier heights 17–18 kcal/mol higher than the reference data, while NKS leads to significantly lower absolute energies for the transition state, with errors for PBE and PBE0 being -8.6 and -8.4 kcal/mol, respectively. In Figure 5 (e) and (f), we show that although the magnitudes of local magnetic moments of PBE NKS calculations remain the same as those from PBE UKS calculations, NKS leads to a further lowering of energy by allowing the noncollinear alignments.

4.3. Cases Stable to Noncollinearity. Finally, we mention cases where no further stabilization is found when the collinear constraint is relaxed. The first example is the reaction barrier of $Cl + H_2 \rightarrow HCl + H$, in which we performed NKS calculations from multiple initial guesses for the transition states with no lower energy SCF solutions found. This example can represent a wide collection of reactions where the transition states, contrary to some misconceptions, do not have significant multi-reference character. Next, we want to make clear that not all multi-reference systems are unstable when spin is allowed to be noncollinear. Test cases we have tried that do not reveal any difference between UKS and NKS include the barrier height of the D_{4h} transition state for automerization of cyclobutadiene (C_4H_4) between rectangular D_{2h} minimum-energy structures,³⁶ as well as the barrier height of the D_{8h} transition state for double-bond shifting in cyclooctatetrane (C_8H_8) between D_{4h} localized double-bond structures.⁴⁶ For these multi-reference systems, both the transition states and the minimum-energy states are stable with respect to the spin orbitals becoming noncollinear. We also tested the dissociation curve of H_2 , where large internuclear separations provide another well-known multi-reference system, and where we were unable to find instability of the UKS solutions. Thus, it is not obvious where the noncollinear relaxation will lower the energy, and readers should be aware that not all multi-reference systems are alike. In fact, analysis of the stability to noncollinear relaxation may provide a useful tool for classifying different kinds of multi-reference character. Because one is unable to predict the stability of a system with respect to noncollinear spin symmetry

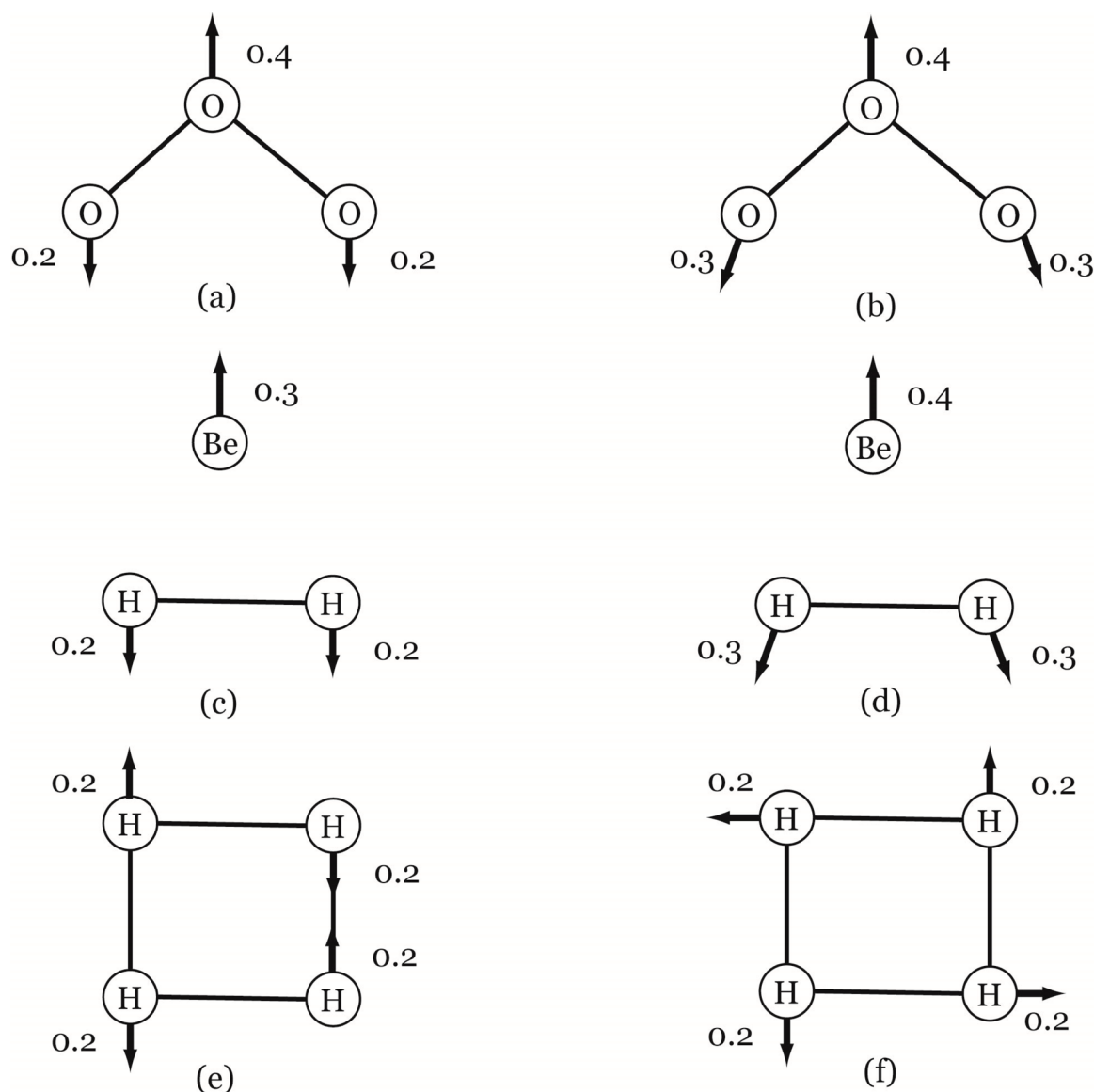


Figure 5. Local spin magnetic moments calculated by PBE: (a) ozone at $\lambda = 0.7$ by UKS with $M_S = 0$, (b) ozone at $\lambda = 0.7$ by NKS with $M_S = 0$, (c) BeH_2 at transition state by UKS with $M_S = 0$, (d) BeH_2 at transition state by NKS with $M_S = 0$, (e) square H_4 by UKS with $M_S = 0$, and (f) square H_4 by NKS with $M_S = 0$.

Table 3. Barrier Heights for H_4 (kcal/mol) Calculated by UKS and NKS with PBE and PBE0 with $M_S = 0$

	UKS	NKS
PBE	116.1	89.5
PBE0	116.8	86.1
ref.	99.1 ^a	

^aFrom ref 37.

breaking beforehand, the safest procedure is to try NKS rather than only UKS to achieve the lowest possible SCF solution.

4. CONCLUSIONS

We have compared UKS and NKS results for dissociation of transition metal oxides as well as barrier heights for multi-reference systems. NKS provides direct and accurate descriptions of the dissociation processes of MnO and NiO , which are highly challenging processes for UKS due to their spin couplings. Stabilization of multi-reference transition states

of ozone, BeH_2 , and H_4 by noncollinear relaxation of Slater determinants leads to different conclusions about the accuracy of exchange–correlation functionals than would be drawn from constrained (“unrestricted”) optimizations.

It is well known that one can use currently available functionals in noncollinear calculations, as is done here and in all the noncollinear references that we cite both here and in ref 26. It is also well known that current functionals are not exact and need further development to achieve good accuracy across the broad spectrum of systems of chemical and physical interest.⁵⁰ Development and assessment of new exchange–correlation functionals intended for multi-reference systems can benefit by taking account of the energy lowering possible with noncollinear spin orbitals. It is difficult to completely decouple the error due to using inexact exchange–correlation functionals from that due to incomplete optimization of the Slater determinant, but one should always bear in mind that assessment of exchange–correlation functionals without the complication of possible errors due to constraints on the

optimization requires the use of the stable and variationally optimized solutions.

AUTHOR INFORMATION

Corresponding Author

*E-mail: truhlar@umn.edu.

Notes

The authors declare no competing financial interest.

ACKNOWLEDGMENTS

This work was supported in part by the Air Force Office of Scientific Research under Grant FA9550-11-1-0078.

REFERENCES

- (1) Kohn, W.; Sham, L. J. *Phys. Rev.* **1965**, *140*, A1133.
- (2) Jacob, C. R.; Reiher, M. *Int. J. Quantum Chem.* **2012**, *112*, 3661.
- (3) Görling, A. *Phys. Rev. A* **1993**, *47*, 2783.
- (4) von Barth, U.; Hedin, L. *J. Phys. C* **1972**, *5*, 1628.
- (5) Rajagopal, A. K.; Callaway, J. *Phys. Rev. B* **1973**, *7*, 1912.
- (6) van Wüllen, C. *J. Comput. Chem.* **2002**, *23*, 779.
- (7) Fukutome, H. *Int. J. Quantum Chem.* **1981**, *20*, 955.
- (8) Löwdin, P.-O.; Mayer, I. *Adv. Quantum Chem.* **1982**, *24*, 79.
- (9) Jiménez-Hoyos, C. A.; Henderson, T. M.; Scuseria, G. E. *J. Chem. Theory Comput.* **2011**, *7*, 2667.
- (10) Sandratskii, L. M.; Goletskii, P. G. *J. Phys. F* **1986**, *16*, L43.
- (11) Kubler, J.; Hock, K.-H.; Sticht, J.; Williams, A. R. *J. Phys. F* **1988**, *18*, 469.
- (12) Hobbs, D.; Kresse, G.; Hafner, J. *Phys. Rev. B* **2000**, *62*, 11556.
- (13) Yamanaka, S.; Yamaki, D.; Shigeta, Y.; Nagao, H.; Yamaguchi, K. *Int. J. Quantum Chem.* **2001**, *84*, 670.
- (14) Soler, J. M.; Artacho, E.; Gale, J. P.; Garcia, A.; Junquera, J.; Ordejón, P.; Sánchez-Portal, D. *J. Phys. Condens. Mat.* **2002**, *14*, 2745.
- (15) Yamanaka, S.; Yamaguchi, K. *Bull. Chem. Soc. Jpn.* **2004**, *77*, 1269.
- (16) Scalmani, G.; Frisch, M. J. *J. Chem. Theory Comput.* **2012**, *8*, 2193.
- (17) Uhl, M.; Sandratskii, L. M.; Kübler, J. *J. Magn. Magn. Mater.* **1992**, *103*, 314.
- (18) Oda, T.; Pasquarello, A.; Car, R. *Phys. Rev. Lett.* **1998**, *80*, 3622.
- (19) Hobbs, D.; Hafner, J.; Spisak, D. *Phys. Rev. B* **2003**, *68*, 014407.
- (20) Longo, R. C.; Noya, E. G.; Gallego, L. J. *Phys. Rev. B* **2005**, *72*, 174409.
- (21) Xie, Y.; Blackman, J. A. *Phys. Rev. B* **2006**, *73*, 214436.
- (22) Sharma, S.; Dewhurst, J. K.; Ambrosch-Draxl, C.; Kurth, S.; Helbig, N.; Pittalis, S.; Shallcross, S.; Nordström, L.; Gross, E. K. U. *Phys. Rev. Lett.* **2007**, *98*, 196405.
- (23) Peralta, J. E.; Scuseria, G. E.; Frisch, M. J. *Phys. Rev. B* **2007**, *75*, 125119.
- (24) Longo, R. C.; Alemany, M. M. G.; Ferrer, J.; Vega, A.; Gallego, L. J. *J. Chem. Phys.* **2008**, *121*, 114315.
- (25) Ruiz-Dias, P.; Dorantes-Davila, J.; Pastor, G. M. *Eur. Phys. J. D* **2009**, *52*, 175.
- (26) Luo, S.; Rivalta, I.; Batista, V.; Truhlar, D. G. *J. Phys. Chem. Lett.* **2011**, *2*, 2629.
- (27) Scalmani, G.; Frisch, M. J. *J. Chem. Theory Comput.* **2012**, *8*, 2193.
- (28) Bulik, I. W.; Scalmani, G.; Frisch, M. J.; Scuseria, G. E. *Phys. Rev. B* **2013**, *85*, 35117.
- (29) Truhlar, D. G. *J. Comput. Chem.* **2007**, *28*, 73.
- (30) Hay, P. J.; Dunning, T.-H.; Goddard, W. A. *J. Chem. Phys.* **1975**, *62*, 3912.
- (31) Laidig, W. D.; Schaefer, H. F., III. *J. Chem. Phys.* **1981**, *74*, 3411.
- (32) Adler-Golden, S. M.; Langhoff, S. R.; Bauschlicher, C. W., Jr.; Carney, G. D. *J. Chem. Phys.* **1985**, *83*, 255.
- (33) Ljubic, I.; Sabljic, A. *J. Phys. Chem. A* **2002**, *106*, 4745.
- (34) Chang, W.-T.; Weng, C.; Goddard, J. D. *J. Phys. Chem. A* **2007**, *111*, 4792.
- (35) Zhao, Y.; Tishchenko, O.; Gour, J. R.; Li, W.; Lutz, J. J.; Piecuch, P.; Truhlar, D. G. *J. Phys. Chem. A* **2009**, *113*, 5786.
- (36) Jiang, W.; Jeffery, C. C.; Wilson, A. K. *J. Phys. Chem. A* **2012**, *116*, 9969.
- (37) Becke, A. D. *J. Chem. Phys.* **2013**, *139*, 021104.
- (38) Kresse, G.; Furthmüller, J. *Comput. Mater. Sci.* **1996**, *6*, 15.
- (39) Kresse, G.; Furthmüller, J. *Phys. Rev. B* **1996**, *54*, 11169.
- (40) Blochl, P. E. *Phys. Rev. B* **1994**, *50*, 17953.
- (41) Paier, J.; Hirschl, R.; Marsman, M.; Kresse, G. *J. Chem. Phys.* **2005**, *122*, 234102.
- (42) Anderson, K.; Malmqvist, P.-Å.; Roos, B. O.; Sadlej, A. J.; Wolinski, K. *J. Phys. Chem.* **1990**, *94*, 5483.
- (43) Adamo, C.; Barone, V. *J. Chem. Phys.* **1999**, *110*, 6158.
- (44) Halgren, T. A.; Lipscomb, W. N. *Chem. Phys. Lett.* **1977**, *49*, 225.
- (45) Perdew, J. P.; Burke, K.; Ernsterhof, M. *Phys. Rev. Lett.* **1996**, *77*, 3865.
- (46) Karadakov, P. B. *J. Phys. Chem. A* **2008**, *112*, 12707.
- (47) Werner, H.-J.; Knowles, P. J.; Knizia, G.; Manby, F. R.; Schütz, M. *WIREs Comput. Mol. Sci.* **2012**, *2*, 242.
- (48) Werner, H.-J.; Knowles, P. J.; Knizia, G.; Manby, F. R.; Schütz, M.; et al. *Molpro*, version 2012.1, a package of ab initio programs. <http://www.molpro.net>.
- (49) Yang, K.; Zheng, J.; Zhao, Y.; Truhlar, D. G. *J. Chem. Phys.* **2010**, *132*, 164117.
- (50) Peverati, R.; Truhlar, D. G. *Phil. Trans. Roy. Soc. A*, in press. DOI: 10.1098/rsta.2012.0476; available online at <http://arxiv.org/abs/1212.0944>.